

Systematics of the Electroweak Plasma at Finite Temperature I

B. J. K. Smith, N. S. Witte and K. C. Hines

School of Physics, University of Melbourne,
Parkville, Vic. 3052, Australia.

Abstract

This paper provides a systematic treatment of the finite temperature field theory which will be required for the subsequent calculation in detail (given in the second paper in this series) of the linear response properties of the electroweak plasma at finite temperature at the one-loop level in the R_ξ gauge. Following a brief summary of the path integral formalism in field theory, the finite temperature theory is introduced with emphasis on the relevant Feynman rules and Matsubara sums. The polarisation tensor for the electroweak plasma is calculated by analysing the appropriate Feynman diagrams. The contributions to the one-loop polarisation tensor are calculated for the tadpole, loop and balloon diagrams in a form suitable for the subsequent investigation of electroweak plasma properties.

1. Introduction

The standard electroweak theory of Glashow, Salam and Weinberg (Glashow 1961; Salam 1968; Weinberg 1967) describes the interacting system of leptons and scalar bosons coupled to the gauge vector bosons W^\pm , Z^0 and γ . Together with the quark sector and gauge bosons of the strong interaction, this theory forms the Standard Model, the foundation of present day elementary particle physics.

A key feature of the standard electroweak theory is the spontaneous symmetry breaking transition, whereby the higher symmetry of the theory is broken through the appearance of a non-zero vacuum expectation value of the scalar field in the theory $\langle 0|\phi|0\rangle \neq 0$. This corresponds to a finite fraction of the scalar field particles residing in the ground state, a phenomenon known as Bose–Einstein condensation. This scalar field, the Higgs field, and this mechanism provide the vector gauge bosons and certain leptons with mass. The symmetry breaking transition also manifests itself as a phase transition in the electroweak plasma, a system of mobile leptons, scalar particles and vector bosons, each coexisting with appropriate density at finite temperatures. So at temperatures greater than some critical value, $T > T_c$, the full symmetry of the theory is restored, i.e. vector bosons become massless.

There are a number of motivations in the study of electroweak plasmas. As a realisation of the symmetry breaking transition and the Higgs mechanism, the electroweak plasma allows aspects of the Standard Model to be formulated, investigated and tested in a more general setting. This system therefore may be

regarded as a generalisation of the more conventional charged plasma interacting purely electrodynamically. The novel features for the electroweak plasma include the finite masses of the W^\pm and Z^0 mediating bosons, as opposed to the massless photon of conventional plasma physics, the effects of Bose condensation of the massive bosons, whereby a macroscopic fraction of these particles reside in the lowest energy state, and the self-interaction effects of non-abelian gauge fields. As the energy scale of the transition is set by the size of the Higgs field vacuum expectation value, the relevant energy or temperature scale is estimated to be 250 GeV. The electroweak transition is thought to be one of the sequence of transitions occurring in the early Universe and determining its consequent evolution. While precise astrophysical implications are uncertain, any progress in understanding the thermodynamics and excitations of the phases at this energy scale would be important in the construction of cosmological models.

The linear response properties of the 0-spin pair plasma at finite temperature both in the presence and absence of a strong uniform magnetic field were studied by Witte and co-workers (1987–90) and the collective properties of the ideal magnetised system were presented. The linear response tensor for both the spin-0 and spin-1 boson/anti-boson plasmas was given by Williams and Melrose (1989).

Ferrer *et al.* (1987, 1988) have calculated the effective potential at high temperature for the electroweak model using two methods. The first method used was an expansion around zero field in the Feynman gauge. The second method was to imbed the gauge conditions in the definitions of the mean values of the fields and expand out the functional determinant. The coefficients of the polynomial representing the functional determinant were related to the coefficients of the high temperature expansion of the effective potential by the Viète theorem. Using conditions on the effective potential, the transition curve for W^\pm condensation has been obtained and the critical temperature calculated. In two later papers (Ferrer *et al.* 1990*a,b*) the effect of the W^\pm condensate on the spectrum of fermions was examined using an iterative approach. It was shown that with increasing temperature, the W^\pm condensate evaporates before the Higgs condensate. There is a mixing between the gauge fields which leads to a redefinition of the gauge fields and the appearance of a massive photon.

The one loop thermodynamic potential was calculated by Kapusta (1990) in the R_ξ gauge using the Viète theorem of Ferrer *et al.* (1988). The phase diagram for the variation of the leptonic chemical potential was shown. An important note was made that the loop expansion is an expansion in powers of the Lagrangian, while the high temperature expansion is an expansion in powers of the interaction and the terms from these two expansions need to be kept to the same order in the approximation.

Kalashnikov *et al.* (1990) calculated the one loop effective potential in the R_ξ gauge using a determinant method with the chemical potentials embedded via non-zero expectation values in the relevant field. These results were compared to those obtained from the unitary gauge and a phase transition curve for W^\pm condensation was given.

As a further complication, Boyd *et al.* (1993) calculated the effective potential for the electroweak model in the unitary gauge and examined the infrared divergences present. They have cast doubt on the validity of the one loop expression, and have used the set of ring diagrams to give a correction to the one loop result.

This gave a phase transition which was more weakly first order than previously obtained and indicated that the baryon asymmetry would not be generated at this transition.

The expressions for the effective potential using the various calculational methods and choices of gauge given above are not in agreement, and further evaluation of the electroweak plasma is required. Thus to date the general topology of the phase boundary of the symmetry breaking phase transition is not known, and the nature and strength of the transition is unclear.

The aim of the present work is to step back from the details of the early Universe and provide a broad general discussion, within the framework of gauge field theory, of the behaviour of the particles involved using the polarisation tensor in the one loop approximation. From the polarisation tensor, the thermodynamics and dispersion relations of the system can be obtained and the consequences of the appearance of an electroweak plasma in the early evolution of the Universe and any phase transitions that the electroweak plasma may undergo can then be evaluated. By using a systematic approach, the set of particles which make the main contribution to the phase transition can be obtained, which gives insight into the development required to extend the calculations.

This paper (designated Paper I) and Paper II (Smith *et al.* 1995, present issue p. 775) to follow will provide the framework for further study of the plasma physics consequences of finite temperature electroweak theory for which the collective interactions typical of the plasma state are of great importance. This point of view will make it possible to formulate a linear many body theory which will be the electroweak analogue of the quantum electrodynamic plasma first studied by Tsytovich (1961). Thus the direction of the work presented here and in Paper II is towards the development of a general theory of the electroweak plasma. Further detailed consideration of the early Universe should await the completion of this development since it is not only the phase transitions which are important for the evolution of the early Universe but the various dissipation processes acting in a plasma may be of even greater significance. The existence of the imaginary parts in the response function of the electroweak plasma to be discussed in Paper II constitutes the first hint for the important concept of such collective dissipation effects in the early Universe.

The present paper (Paper I) has as its aim the determination of all contributions to the polarisation tensor of the electroweak plasma at the one-loop level. The generic forms for the polarisation tensor for the tadpole, loop and balloon diagrams are given in equations (81), (94) and (101) respectively. An example of the procedure used to obtain the polarisation tensor for a specific diagram from the generic form is given at the end of Section 5.3. Paper II will contain a detailed development of this polarisation tensor, including real and imaginary parts, in a form that will be used to calculate the physical properties of the electroweak plasma. The correspondence between each diagram and the equations and functions used to describe it is given in Table 5 of Paper II.

2 Lagrangian

2.1 Generating Functional

Classical field theory can be quantised using two equivalent approaches. The canonical formalism involves taking the variables of the system to be operators that satisfy canonical commutation relations. The time evolution of the system is obtained from the quantised Hamiltonian and the transition amplitude for the system changing from an initial state to a final state can be calculated.

The path integral formalism is standard and appears in a number of textbooks, for example Cheng and Li (1988), Pokorski (1987) and Bailin and Love (1986). This formalism involves expressing the transition amplitude as a functional integral over all possible paths between the final and initial states. Each possible path is weighted by the probability of that path being taken, which is the exponential of i times the action.

Using the path integral formalism, the vacuum-to-vacuum transition amplitude in the presence of a source $J(x)$ is given by the generating functional

$$W[J] \sim \int [d\phi] \exp \left\{ i \int d^4x [\mathcal{L}(\phi(x)) + J(x)\phi(x)] \right\}. \quad (1)$$

The vacuum matrix elements or Green functions are generated by functional differentiation of equation (1):

$$G^{(n)}(x_1, \dots, x_n) = \frac{\delta^n W[J]}{\delta J(x_1) \dots \delta J(x_n)} \Big|_{J=0} \quad (2)$$

The Green function in momentum space is defined by the Fourier transform of the particular Green function in configuration space

$$\begin{aligned} G^{(n)}(p_1, \dots, p_n) &= (2\pi)^4 \delta(p_1 + \dots + p_n) \\ &= \int d^4x_1 \dots \int d^4x_n \exp [i(p_1 \cdot x_1 + \dots + p_n \cdot x_n)] G^{(n)}(x_1, \dots, x_n). \end{aligned} \quad (3)$$

The connected Green functions are obtained by functional differentiation of the connected generating functional

$$Z[J] = \ln W[J], \quad (4)$$

while the one particle irreducible Green functions are obtained by functional differentiation of the effective action generating functional

$$\Gamma(\phi_c) = Z[J] - \int d^4x J(x)\phi_c(x), \quad (5)$$

where $\phi_c(x)$ is the classical field. The classical field is defined as the field which minimises

$$\Gamma(\phi) + \int d^4x J(x)\phi(x).$$

The classical field can be defined in an equivalent manner by

$$\frac{\delta \Gamma(\phi)}{\delta \phi} \Big|_{\phi=\phi_c} = -J(x). \quad (6)$$

Using the relationship between the Green functions and the generating functional, an expansion is made for the generating functional

$$W[J] = \sum_{n=0}^{\infty} \frac{1}{n!} \int d^4x_1 \dots \int d^4x_n G^{(n)}(x_1, \dots, x_n) J(x_1) \dots J(x_n), \quad (7)$$

which is equivalent to the standard Taylor expansion of functions.

We see later in the interacting field theory that the connected Green functions, obtained from the connected generating functional, are represented by Feynman diagrams that are connected. The one particle interacting Green functions, obtained from the effective action, are represented by Feynman diagrams that are connected and that cannot be disconnected by cutting a single internal line. The one particle interacting Green functions have the factors associated with external legs divided out.

Each generating functional can be evaluated exactly only if it involves Gaussian integrals. For an interacting gauge field theory, a perturbative expansion is made in terms of a small parameter. The Lagrangian is split into interacting and non-interacting parts

$$\mathcal{L} = \mathcal{L}_0 + \mathcal{L}_I, \quad (8)$$

where the interacting Lagrangian \mathcal{L}_I is proportional to a small parameter, λ .

The generating functional is written as

$$W[J] = \left[\exp \int d^4x \mathcal{L}_I \left(\frac{\delta}{\delta J} \right) \right] W_0[J], \quad (9)$$

where

$$W_0[J] = \int [d\phi] \exp \left[\int d^4x (\mathcal{L}_0 + J\phi) \right] \quad (10)$$

is the generating functional in the absence of interactions.

The exponential is expanded in a power series to give

$$W[J] = \left\{ 1 + \int d^4x \mathcal{L}_I \left(\frac{\delta}{\delta J} \right) + \dots \right\} W_0[J]. \quad (11)$$

Equation (11) can be represented by Feynman diagrams. For the 2-point Green function or propagator we have

$$\text{-----} = \text{-----} + \text{---} \text{ (shaded blob) } \text{---} + \text{---} \text{ (shaded blob) } \text{---} \text{ (shaded blob) } \text{---} + \dots \quad (12)$$

where the full field propagator is represented by the double dashed line, the free field propagator by the single dashed line and the one particle irreducible diagrams by the shaded blob. The diagrams form a geometric series which is summed to give the Dyson equation

$$\mathcal{D} = \frac{1}{\mathcal{D}_0^{-1} - \Sigma}, \quad (13)$$

or equivalently

$$\mathcal{D} = \mathcal{D}_0 + \mathcal{D}_0 \Sigma \mathcal{D}, \quad (14)$$

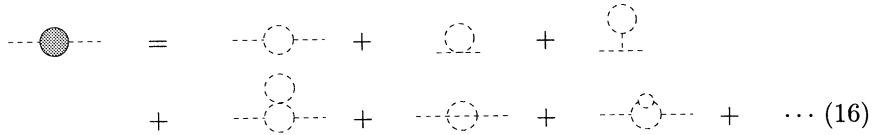
where \mathcal{D} is the full propagator, \mathcal{D}_0 is the free propagator and Σ is the self energy operator given by the one particle irreducible diagrams with the external legs truncated. Hence the full propagator can be obtained by a study of the one particle irreducible diagrams.

Equation (13) can be inverted to give

$$\mathcal{D}^{-1} = \mathcal{D}_0^{-1} - \Sigma, \quad (15)$$

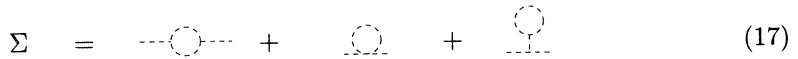
which shows that in the presence of interactions, the propagator shifts from the bare propagator to the full propagator with the magnitude of the shift determined by the self energy operator.

The one particle irreducible diagrams are defined as those diagrams that cannot be broken into two separate diagrams by cutting a single internal line. Hence the one particle irreducible diagrams are given by



The diagrams shown in equation (16) correspond to the self interactions between a particular boson. For the electroweak theory considered in this work, the particles propagating in the internal parts of the diagrams will be determined from the electroweak Lagrangian.

Since \mathcal{L}_I is proportional to λ , each loop of a diagram contributes λ^2 to the final results, due either to two 3-vertices or one 4-vertex. At the lowest order, the self energy operator is given by the diagrams containing one loop. Expressed in terms of Feynman diagrams, the one loop self energy operator is given by



The diagrams that contribute to the self energy operator for each particle depend on the interactions between the particles given by the Lagrangian. Each diagram is divided by a symmetry factor \mathcal{S} given in Cheng and Li (1988), which corresponds to the number of permutations of internal lines that can be made for fixed vertices. There is an additional minus sign for each closed fermion loop or ghost loop.

The perturbative expansion of the generating functional in powers of \mathcal{L}_I used in the path integral formalism is shown to be equivalent to the Wick expansion of the transition amplitude used in the canonical quantisation method in Cheng and Li (1988) and Bailin and Love (1986).

2.2 Finite Temperature Theory

2.2.1 Imaginary-Time Formalism

The imaginary-time formalism uses the correspondence between the partition function at finite temperature and the generating functional of zero-temperature theory given in Bernard (1974). This work is summarised and extended in a number of reference works on this subject, for example, Morley and Kislinger (1979), Kapusta (1981) and Landsman and Van Weert (1987).

The statistical thermodynamics of a system at finite temperature is given by the partition function

$$Z = \text{tr } e^{-\beta(H+\mu N)}, \quad (18)$$

where H is the Hamiltonian governing the behaviour of the system, N is the number operator, μ is the chemical potential and $\beta = T^{-1}$ is the inverse temperature.

The partition function for bosons can be written as a summation over the eigenstates $\phi(x)$ of the system

$$Z = \sum_{\phi(x)} \langle \phi(x), t=0 | e^{-\beta(H+\mu N)} | \phi(x), t=0 \rangle. \quad (19)$$

The partition function for fermions will be examined later.

For vacuum field theory, the transition amplitude for state $|\phi''(x), t''\rangle$ going to $|\phi'(x), t'\rangle$ is given by the path integral

$$\begin{aligned} & \langle \phi''(x), t=0 | e^{-i(H+\mu N)(t''-t')} | \phi'(x), t=0 \rangle \\ & \sim \int \mathcal{D}\phi \int \mathcal{D}\pi \exp i \int_{t'}^{t''} dt \int d^3x \left(\pi \frac{\partial \phi}{\partial t} - H(\pi, \phi) - \mu N(\pi, \phi) \right), \end{aligned} \quad (20)$$

where $\phi(x)$ represents the field and π represents the associated momentum. The correspondence with finite temperature field theory is achieved by introducing the variable

$$\tau = it, \quad (21)$$

and using the limits of integration $t' = 0$, $t'' = -\beta$. Then we get

$$\begin{aligned} & \langle \phi''(x), t=0 | e^{-\beta(H+\mu N)} | \phi'(x), t=0 \rangle \\ & \sim \int \mathcal{D}\phi \int \mathcal{D}\pi \exp i \int_0^\beta d\tau \int d^3x \left(i\pi \frac{\partial \phi}{\partial \tau} - H(\pi, \phi) - \mu N(\pi, \phi) \right). \end{aligned} \quad (22)$$

This expression can be made identical to the transition amplitude given in equation (19) by imposing the condition

$$|\phi''(x), t=0\rangle = |\phi'(x), t=0\rangle = |\phi(x), t=0\rangle, \quad (23)$$

and summing over the eigenstates. This gives the result for the partition function

$$Z \sim \int_{\text{periodic}} \mathcal{D}\phi \int \mathcal{D}\pi \exp i \int_0^\beta dt \int d^3x \left(i\pi \frac{\partial \phi}{\partial \tau} - H(\pi, \phi) - \mu N(\pi, \phi) \right). \quad (24)$$

The π integration can be carried out explicitly to give

$$Z \sim \int_{\text{periodic}} \mathcal{D}\phi \exp i \int_0^\beta dt \int d^3x \mathcal{L}(\phi, \bar{\partial}_\mu \phi), \quad (25)$$

where

$$\bar{\partial}_\mu \phi \equiv \left(i \frac{\partial \phi}{\partial \tau}, \nabla \phi \right). \quad (26)$$

As $\phi(x, \tau)$ is periodic in the interval $0 < \tau < \beta$, an expansion can be made in a Fourier series

$$\phi(x, \tau) = \frac{1}{\beta} \sum_n \int \frac{d^3 \mathbf{q}}{(2\pi)^3} e^{i\mathbf{k} \cdot \mathbf{x}} e^{i\omega_n \tau} \varphi_n(\mathbf{k}), \quad (27)$$

where $\omega_n = 2\pi n/\beta$.

The partition function for fermions is defined with $|\phi(x), t=0\rangle$ as the final state in the sum as the fields are anti-periodic. This gives a summation over the anti-periodic boundary conditions and an expansion in Fourier series with $\omega_n = (2n+1)\pi/\beta$.

The integration over eigenstates, as it stands, does not allow for the fact that some eigenstates are equivalent as they are connected by a gauge transformation. The Faddeev–Popov Lagrangian is included into the electroweak theory and this Lagrangian is expressed in terms of ghost fields. These fields do not correspond to physical particles but are a mathematical construct used so that a perturbation series can be generated. The ghost fields are defined to be anti-commuting variables and the anti-symmetry means that there is a minus sign for a diagram with a closed ghost loop, the same prescription as that for a closed fermion loop. The spin statistics of the ghost particles are the same as for bosons.

The imaginary-time formalism is structured so that the perturbation expansion generated can be represented by the same diagrams as in the vacuum theory, a point made in Landsman and Van Weert (1987). The difficulty that occurs is that the propagators have imaginary time arguments and an analytic continuation is required to give physically meaningful results.

2.2.2 Finite Temperature Feynman Rules

The finite temperature Feynman rules follow from the manipulations used in the imaginary-time formalism to obtain the correspondence between the vacuum theory and the finite temperature theory. Following Bernard (1974) and Landsman and Van Weert (1987) these rules are obtained from the vacuum Feynman rules with the substitutions

$$\tilde{G}(q_1, \dots, q_n) \rightarrow (-i)^n \tilde{G}^{(E)}(q_1, \dots, q_n), \quad (28)$$

$$\int \frac{d^4 q}{(2\pi)^4} \frac{1}{i} \rightarrow \frac{1}{\beta} \sum_N \int \frac{d^3 \mathbf{q}}{(2\pi)^3}, \quad (29)$$

$$i(2\pi)^4 \delta(q_1 + \dots + q_n) \rightarrow \beta \delta_{\omega_1 + \dots + \omega_n} (2\pi)^3 \delta^{(3)}(q_1 + \dots + q_n), \quad (30)$$

$$q^0 \rightarrow i\omega_n + \mu \begin{cases} \omega_n = 2n\pi T & \text{Boson,} \\ \omega_n = (2n+1)\pi T & \text{Fermion.} \end{cases} \quad (31)$$

Equations (28) and (29) together imply that the propagators lose a factor of $-i$ and equation (30) implies that at each vertex effectively a factor of i disappears. Landsman and Van Weert (1987) gave a specification for equation (29) where β multiplies the sum, an obvious typographic error.

The statistical and symmetry factors of vacuum theory are used unchanged in the finite temperature formalism, along with the standard renormalisation prescriptions.

2.2.3 Matsubara Sum

At zero temperature, conservation of momentum is applied at each vertex and an integration is performed over any undetermined 4-momenta. For finite temperature the same type of procedure is applied and as can be seen from equation (27), integration is performed over any undetermined 3-momenta and a summation is performed over any undetermined ω_n . The summation is known as the Matsubara summation and can be performed by an analytic continuation of the time contour and the standard Regge pole analysis detailed in Fetter and Walecka (1971).

When the particle with undetermined momentum is a boson, periodic boundary conditions are required. The summand is multiplied by an analytic function with poles of residue 1 at the even integers and the contour integration is over this combination. The Matsubara sum for a boson with component $q^0 = i2N\pi T + \mu$ is

$$\begin{aligned} \frac{1}{\beta} \sum_N f(q^0 = i2N\pi T + \mu) \\ = \int_{C_+} \frac{dz}{2\pi i} [n(z - \mu)f(z) + n(z + \mu)f(-z)] + \int_{-i\infty}^{+i\infty} \frac{dz}{2\pi i} f(z), \end{aligned} \quad (32)$$

which is given in a number of references including Morley and Kislinger (1979), Landsman and Van Weert (1987) and Kapusta (1989).

When the particle with undetermined momentum is a fermion, anti-periodic boundary conditions are required and the same procedure is followed. The Matsubara sum for a fermion with component $q^0 = i(2N + 1)\pi T + \mu$ is

$$\begin{aligned} \frac{1}{\beta} \sum_N f(q^0 = i(2N + 1)\pi T + \mu) \\ = - \int_{C_+} \frac{dz}{2\pi i} [n(z - \mu)f(z) + n(z + \mu)f(-z)] + \int_{-i\infty}^{+i\infty} \frac{dz}{2\pi i} f(z), \end{aligned} \quad (33)$$

where

$$n(x) = \begin{cases} [e^{\beta x} - 1]^{-1} & \text{Boson,} \\ [e^{\beta x} + 1]^{-1} & \text{Fermion.} \end{cases} \quad (34)$$

The presence of the temperature distribution functions is anticipated as we started with the partition function of thermodynamics.

These formulae are valid for any function $f(z)$ which is analytic in the neighbourhood of the imaginary axis and has the property that the product $f(z)e^{-\beta z}$ vanishes sufficiently fast at infinity. The contour C_+ circumscribes *clockwise* all singularities of the functions $f(z)$ and $f(-z)$ in the right half plane but none of the singularities of the Bose-Einstein/Fermi-Dirac distribution functions at the Matsubara frequencies. The integral over the C_+ contour is the finite temperature dependent part of the Matsubara sum.

The second integral in equation (32) or (33) gives the zero temperature part of the Matsubara sum. A Wick rotation is performed on this integral. In specifying the direction of rotation, a specific real axis integration is defined leading to $\pm i\varepsilon$ in the denominator. As detailed in Section 2.2.2, each propagator loses $-i$ and each

vertex loses i . Since a vertex and propagator will always be paired together in a Feynman diagram, the zero temperature part of a diagram specified through finite temperature field theory will give the same contribution as that obtained from the zero temperature vacuum theory.

The first contour integral of equations (32) or (33) gives the temperature dependent part of the diagram, hence only this part will be considered in calculating the finite temperature parts of the polarisation tensor.

From complex variable theory, the Cauchy theorem states

$$\int_C f(z)dz = 2\pi i \sum_{j=1}^m \text{Res}_{z=z_j} f(z), \quad (35)$$

where the integral is taken *counter-clockwise* around the poles, and $f(z)$ has m poles at z_1, \dots, z_m . As C_+ encloses poles in a clockwise direction, for the finite temperature parts

$$\frac{1}{\beta} \sum_N f(q^0 = i2N\pi T + \mu) = - \sum_{j=1}^m \text{Res}_{z=z_j} [n(z - \mu)f(z) + n(z + \mu)f(-z)], \quad (36)$$

$$\frac{1}{\beta} \sum_N f(q^0 = i(2N + 1)\pi T + \mu) = + \sum_{j=1}^m \text{Res}_{z=z_j} [n(z - \mu)f(z) + n(z + \mu)f(-z)]. \quad (37)$$

We can combine the Matsubara sum for the odd and even statistics by introducing a factor

sign	type of contour
–	boson,
–	ghost,
+	fermion,

which takes account of the signs in equations (36) and (37). This is similar to the spin statistics factor which is

sign	type of closed loop
+	boson,
–	ghost,
–	fermion.

The general distribution function

$$F(z, \mu) = n(z - \mu) + n(z + \mu). \quad (38)$$

is defined where the number distribution function $n(x)$ will be a Bose–Einstein distribution function for a boson or ghost particle and a Fermi–Dirac distribution function for a fermion.

2.3 Analytic Continuation

Any function obtained under the imaginary-time formalism is defined at a discrete set of points in the imaginary plane, given by $q^0 = i\omega_n + \mu$. This result must be

analytically continued to the real axis by the prescription given in Landsman and Van Weert (1987)

$$\mathcal{F}(\omega, \mathbf{q}) = \mathcal{F}(q^0 = i\omega_n + \mu, \mathbf{q}) \Big|_{q^0 \rightarrow \omega + i\varepsilon} \quad (39)$$

The infinitesimal part $+i\varepsilon$ corresponds to imposing the causal condition on the polarisation tensor. The analytic continuation procedure is well-defined only when analytic continuation is performed after the Matsubara summation has been done.

The notation used here is

Imaginary time function:	$\mathcal{F}(q^0, \mathbf{q})$	where $q^2 = q^{02} - \mathcal{Q}^2$,
Analytic function:	$\mathcal{F}(\omega, \mathbf{q})$	where $q^2 = \omega^2 - \mathcal{Q}^2$,

where $\mathcal{Q} \equiv |\mathbf{q}|$.

2.4 Renormalisation and Running Coupling

For a zero temperature gauge field theory, calculation of Feynman diagrams involving loops will yield infinities due to ultra-violet divergences. This is due to the fact that there is no large scale momentum cutoff, the variable in the momentum integration ranging from zero to infinity. In order to remove the infinity and obtain a meaningful calculation, renormalisation is required.

The Lagrangian for the theory contains bare parameters, i.e. parameters in the absence of an interaction. Since it is not possible to turn off the interaction for a gauge field theory the bare parameters are not measurable. The renormalisation scheme consists of isolating the infinity in the integration and canceling this against the unrenormalised quantities to give a finite result.

The finite temperature calculation for a particular Feynman diagram has a loop integration composed of two parts, the temperature-independent integral and the finite temperature integral. The finite temperature integral is ultra-violet convergent due to the Bose-Einstein/Fermi-Dirac distribution functions, which are proportional to $e^{-p/T}$ for large momenta. The temperature-independent integral is identical to the zero temperature integral for that diagram and as such needs to be renormalised. The renormalisation procedure is well-defined and can be performed in a consistent manner for the standard electroweak model, for example as in Cole (1985) or Aoki *et al.* (1982). The finite temperature results shown here will depend on the standard renormalised parameter.

The renormalisation scheme used has some arbitrariness related to the choice of kinematic points in defining the physical parameters such as the mass and the coupling constants. Since the physics of the system should not be dependent on the choice of kinematic points then there should exist relationships between the physical parameters based on transformations of the renormalisation conditions. These relationships are given by the renormalisation equation. In particular, the coupling constant in any renormalisation scheme is energy dependent, a function of the subtraction point used.

Further work that could be considered is to examine how the the presence of finite temperature in the calculations changes the functionality of the running coupling constants or conversely, how the running coupling constant changing with energy changes the calculations at finite temperature. That is, given that the running coupling constant is energy dependent it could also be temperature dependent.

3 Electroweak Model

The Lagrangian density for the standard electroweak theory (Glashow 1961, Salam 1968, Weinberg 1967) in the manifestly renormalisable R_ξ gauge will be described by separate sections as follows:

$$\begin{aligned}\mathcal{L} = & \mathcal{L}_{\text{Higgs}} + \mathcal{L}_{\text{Gauge Fixing}} + \mathcal{L}_{\text{Gauge Kinetic}} \\ & + \mathcal{L}_{\text{Ghost}} + \mathcal{L}_{\text{Fermion Kinetic}} + \mathcal{L}_{\text{Yukawa}}.\end{aligned}\quad (40)$$

The Higgs sector of the Lagrangian is

$$\mathcal{L}_{\text{Higgs}} = (D^\mu \Phi)^\dagger (D_\mu \Phi) - V(\Phi), \quad (41)$$

where the Higgs sector fields are

$$\Phi = v + \sqrt{\frac{1}{2}} \begin{bmatrix} G_1 + iG_2 \\ H + iG^0 \end{bmatrix}, \quad (42)$$

$$v = \begin{bmatrix} 0 \\ v \end{bmatrix}, \quad (43)$$

$$V(\Phi) = m^2 \Phi^\dagger \Phi + \frac{1}{16} \lambda (\Phi^\dagger \Phi)^2, \quad (44)$$

and the covariant derivative is

$$D_\mu \Phi = \left(\partial_\mu + \frac{1}{2} i g' B_\mu + \frac{1}{2} i g W_\mu^a \tau^a \right) \Phi. \quad (45)$$

The gauge kinetic part of the Lagrangian is

$$\mathcal{L}_{\text{Gauge Kinetic}} = -\frac{1}{4} F_{\mu\nu}^a F^{\mu\nu a} - \frac{1}{4} G_{\mu\nu} G^{\mu\nu}, \quad (46)$$

where the field strength tensors are

$$F_{\mu\nu}^a = \partial_\mu W_\nu^a - \partial_\nu W_\mu^a - g \epsilon^{abc} W_\mu^b W_\nu^c, \quad (47)$$

$$G_{\mu\nu} = \partial_\mu B_\nu - \partial_\nu B_\mu. \quad (48)$$

The fermion kinetic part of the Lagrangian is

$$\mathcal{L}_{\text{Fermion Kinetic}} = \bar{e}_R i \gamma^\mu D_\mu e_R + \bar{\phi}_L i \gamma^\mu D_\mu \phi, \quad (49)$$

where the left-handed field is

$$\phi_L = \begin{bmatrix} \nu_e \\ e^- \end{bmatrix}, \quad (50)$$

and the right-handed field is e_R . The covariant derivatives are

$$D_\mu \phi_L = \left(\partial_\mu + \frac{1}{2} i g \tau^a W_\mu^a - \frac{1}{2} i g' B_\mu \right) \phi_L, \quad (51)$$

$$D_\mu e_R = \left(\partial_\mu - \frac{1}{2} i g' B_\mu \right) e_R. \quad (52)$$

The Yukawa coupling is

$$\mathcal{L}_{\text{Yukawa}} = -G_l (\bar{\phi}_L \Phi e_R + \bar{e}_R \Phi \phi_L), \quad (53)$$

where G_l is the Yukawa coupling constant.

The gauge fixing term for the R_ξ gauge is

$$\mathcal{L}_{\text{Gauge Fixing}} = -\frac{1}{2\xi} (\partial^\mu W_\mu^a - \frac{1}{2}\xi g v G^a)^2 - \frac{1}{2\xi} (\partial^\mu B_\mu - \frac{1}{2}\xi g' v H)^2. \quad (54)$$

The ghost part of the Lagrangian is

$$\mathcal{L}_{\text{Ghost}} = \partial^\mu \eta^{*a} (\partial_\mu \eta^a + i g \epsilon^{abc} \eta^b W_\mu^c) \quad (55)$$

$$- \xi g^2 \eta^{*a} \eta^b v^\dagger T^a T^b, \quad (56)$$

where

$$T^a = \begin{cases} \tau^a & \text{for } a = 1, 2, 3, \\ g'/g & \text{for } a = 4, \end{cases} \quad (57)$$

$$\epsilon^{abc} = 0 \quad \text{for } a \text{ or } b \text{ or } c = 4. \quad (58)$$

4 The Polarisation Tensor

4.1 Definition of the Polarisation Tensor

The self-energy operator was defined by equations (13) and (15). For gauge bosons propagating in the external legs of the Feynman diagram the same procedure is used. The shift in the propagator is expressed in terms of the polarisation tensor

$$\mathcal{D}_{\mu\nu}^{-1} = \mathcal{D}_{0\mu\nu}^{-1} - \Pi_{\mu\nu}, \quad (59)$$

and the polarisation tensor for a particular gauge boson is given by the one particle irreducible diagrams with that gauge boson in the external legs.

4.2 Symmetries of the Polarisation Tensor

The polarisation tensor for a propagating particle should reflect the symmetries of the physical situation. The symmetry requirements on the polarisation tensor quoted here follow Melrose and McPhedran (1993).

4.2.1 Reality Condition

The analytic polarisation tensor $\Pi_{\mu\nu}(\omega, \mathbf{q})$ is defined in Fourier space and hence has real and imaginary parts. The reality condition

$$\Pi_{\mu\nu}^*(\omega, \mathbf{q}) = \Pi_{\mu\nu}(-\omega, -\mathbf{q}), \quad (60)$$

where the star indicates a complex conjugate, must hold for the polarisation tensor. This condition ensures that a real quantity is obtained when the polarisation tensor in Fourier space is inverted to give the polarisation tensor in space and time.

4.2.2 Hermitean and Anti-Hermitean Parts

The polarisation tensor can be separated into hermitean and anti-hermitean parts to give

$$\Pi_{\mu\nu}(\omega, \mathbf{q}) = \Pi_{\mu\nu}^H(\omega, \mathbf{q}) + \Pi_{\mu\nu}^A(\omega, \mathbf{q}), \quad (61)$$

where the hermitean and anti-hermitean parts are defined by

$$\Pi_{\mu\nu}^H(\omega, \mathbf{q}) = \frac{1}{2} [\Pi_{\mu\nu}(\omega, \mathbf{q}) + \Pi_{\nu\mu}^*(\omega, \mathbf{q})], \quad (62)$$

$$\Pi_{\mu\nu}^A(\omega, \mathbf{q}) = \frac{1}{2} [\Pi_{\mu\nu}(\omega, \mathbf{q}) - \Pi_{\nu\mu}^*(\omega, \mathbf{q})]. \quad (63)$$

The anti-hermitean part describes the dissipative processes occurring in the plasma while the hermitean part describes the non-dissipative processes. For a symmetric tensor

$$\Pi_{\mu\nu}(\omega, \mathbf{q}) = \Pi_{\nu\mu}(\omega, \mathbf{q}), \quad (64)$$

then

$$\Pi_{\mu\nu}^H(\omega, \mathbf{q}) = \text{Re } \Pi_{\mu\nu}(\omega, \mathbf{q}), \quad (65)$$

$$\Pi_{\mu\nu}^A(\omega, \mathbf{q}) = i \text{Im } \Pi_{\mu\nu}(\omega, \mathbf{q}). \quad (66)$$

4.2.3 Onsager Relations

The Onsager relations describe the required behaviour of the polarisation tensor by considering the time-reversal properties of the equations of mechanics. For particles in a magnetic field, the equation of motion is

$$\frac{d\mathbf{p}}{dt} = q_c(\mathbf{E} + \mathbf{v} \times \mathbf{B}), \quad (67)$$

where q_c is the charge on the particle. The equation of motion is unchanged under time-reversal when the direction of both the magnetic field and the direction of the momentum are also reversed.

The anti-hermitean part of the polarisation tensor is an odd function under time-reversal reflecting the fact that it describes dissipative processes. The hermitean part of the polarisation tensor describes non-dissipative processes and is an even function under time-reversal. Hence we have

$$\Pi_{ij}^H(\omega, \mathbf{q}) \Big|_B = \Pi_{ij}^H(-\omega, \mathbf{q}) \Big|_{-B}, \quad (68)$$

$$\Pi_{ij}^A(\omega, \mathbf{q}) \Big|_B = -\Pi_{ij}^A(-\omega, \mathbf{q}) \Big|_{-B}. \quad (69)$$

These relations can be combined using the reality conditions to give the standard form of the Onsager relations

$$\Pi_{ij}(\omega, \mathbf{q}) \Big|_B = \Pi_{ji}(\omega, -\mathbf{q}) \Big|_{-B}. \quad (70)$$

The Onsager relations relate to the spatial sector of the polarisation tensor because the time-reversal symmetry is dependent on the equations of motion of the propagating particle.

4.2.4 Causality

The analytic continuation used in obtaining the analytic polarisation tensor, given in Section 2.3, applies a causal condition to the polarisation tensor. That is, the

polarisation tensor at a given time t can only depend on interactions occurring at earlier times. The causal condition leads to a dependence between the real and imaginary parts of the polarisation tensor given by the Kramers–Kronig relations specified in Melrose and McPhedran (1993) and Jackson (1975)

$$\operatorname{Re} \Pi_{\mu\nu}(\omega, \mathbf{q}) = \frac{1}{\pi} \oint_{-\infty}^{+\infty} d\omega' \frac{\operatorname{Im} \Pi_{\mu\nu}(\omega', \mathbf{q})}{\omega' - \omega}, \quad (71)$$

$$\operatorname{Im} \Pi_{\mu\nu}(\omega, \mathbf{q}) = \frac{1}{\pi} \oint_{-\infty}^{+\infty} d\omega' \frac{\operatorname{Re} \Pi_{\mu\nu}(\omega', \mathbf{q})}{\omega' - \omega}, \quad (72)$$

where the integration is a principal value integration.

Hence the real and imaginary parts are dependent on each other; for example, when the analytic form of the real part of the polarisation tensor is known, the imaginary part can be calculated.

5 Contributions to the One-loop Polarisation Tensor

5.1 Loop Expansion

The diagrammatic expansion of the generating functional in terms of Feynman diagrams used for zero temperature vacuum theory can be carried over to the finite temperature theory. At lowest order the self-energy is given by diagrams containing one loop. These types of diagrams can be constructed from either two 3-vertices and two propagators (the loop and balloon diagrams) or one 4-vertex and one propagator (the tadpole diagram).

The diagrams needed for the calculation of the photon polarisation tensor to e^2 order are

$$\begin{array}{c} \gamma \\ \bullet \\ \gamma \end{array} = e \begin{array}{c} \gamma \\ \bigcirc \\ \gamma \end{array} e + W \begin{array}{c} \gamma \\ \text{star} \\ W \end{array} + W \begin{array}{c} \gamma \\ \text{star} \\ G \end{array} + G \begin{array}{c} \gamma \\ \text{star} \\ G \end{array} + \eta \begin{array}{c} \gamma \\ \text{star} \\ \eta \end{array} + \begin{array}{c} \gamma \\ \text{star} \\ W \end{array} + \begin{array}{c} \gamma \\ \text{star} \\ G \end{array}$$

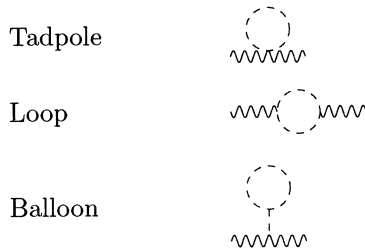
The diagrams needed for the calculation of the Z boson polarisation tensor to g^2 order are

$$\begin{array}{c} Z^0 \\ \bullet \\ Z^0 \end{array} = \nu \begin{array}{c} Z^0 \\ \bigcirc \\ \nu \end{array} + e \begin{array}{c} Z^0 \\ \bigcirc \\ e \end{array} + W \begin{array}{c} Z^0 \\ \text{star} \\ W \end{array} + Z \begin{array}{c} Z^0 \\ \text{star} \\ H \end{array} + W \begin{array}{c} Z^0 \\ \text{star} \\ G \end{array} + G^0 \begin{array}{c} Z^0 \\ \text{star} \\ H \end{array} + G \begin{array}{c} Z^0 \\ \text{star} \\ G \end{array} \\ + \eta \begin{array}{c} Z^0 \\ \text{star} \\ \eta \end{array} + \begin{array}{c} Z^0 \\ \text{star} \\ W \end{array} + \begin{array}{c} Z^0 \\ \text{star} \\ G \end{array} + \begin{array}{c} Z^0 \\ \text{star} \\ G^0 \end{array} + \begin{array}{c} Z^0 \\ \text{star} \\ H \end{array} + \begin{array}{c} Z^0 \\ \text{star} \\ W \end{array} + \begin{array}{c} Z^0 \\ \text{star} \\ Z \end{array} \\ + \begin{array}{c} Z^0 \\ \text{star} \\ H \end{array} + \begin{array}{c} Z^0 \\ \text{star} \\ G^0 \end{array} + \begin{array}{c} Z^0 \\ \text{star} \\ H \end{array} + \begin{array}{c} Z^0 \\ \text{star} \\ \eta \end{array} + \begin{array}{c} Z^0 \\ \text{star} \\ \eta^Z \end{array} + \begin{array}{c} Z^0 \\ \text{star} \\ e \end{array}$$

The diagrams needed for the calculation of the W boson polarisation tensor to g^2 order are

$$\begin{aligned}
 \text{Diagram 1} &= e \text{Diagram 2} + W \text{Diagram 3} + W \text{Diagram 4} + \gamma \text{Diagram 5} + Z \text{Diagram 6} + W \text{Diagram 7} + G \text{Diagram 8} \\
 &+ G \text{Diagram 9} + \eta \text{Diagram 10} + \eta \text{Diagram 11} + \gamma \text{Diagram 12} + Z \text{Diagram 13} + W \text{Diagram 14} + G \text{Diagram 15} \\
 &+ G \text{Diagram 16} + H \text{Diagram 17} + \bar{H} \text{Diagram 18} + \bar{H} \text{Diagram 19} + Z \text{Diagram 20} + \bar{H} \text{Diagram 21} \\
 &+ \bar{H} \text{Diagram 22} + \bar{H} \text{Diagram 23} + \eta \text{Diagram 24} + \eta \text{Diagram 25} + \bar{H} \text{Diagram 26}
 \end{aligned}$$

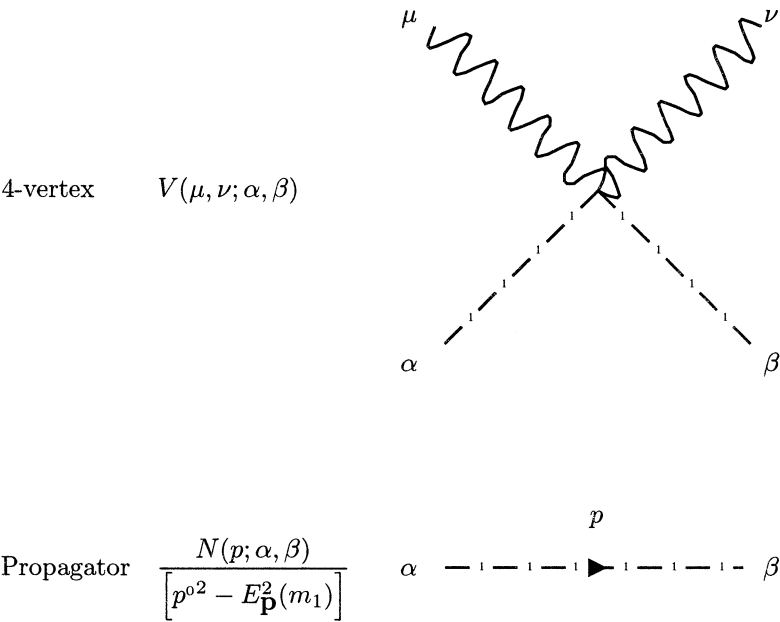
Examples of the generic type of diagrams for gauge bosons propagating in the external legs are



This section gives the general result for the finite temperature contributions of the three distinct Feynman diagrams to the one-loop polarisation tensor—tadpole, loop and balloon. The contribution to the polarisation tensor depends on the contraction of the vertex factors and the propagators for each of these diagrams.

5.2 Tadpole

The tadpole diagram contains a 4-vertex and a propagator



where the external legs of the diagram are taken to be gauge bosons. The notation used is that the particle propagating around the loop is labeled with a “1” on the line and propagates with 4-momentum p , mass m_1 and chemical potential μ_1 . The propagator for any particle can be expressed either directly in the form shown above, or in the case of gauge bosons as the sum of two parts where each part is in the form shown above. The list of all the propagators in the imaginary-time formalism of finite temperature field theory is given in Appendix A.6.

The vertex and propagator are combined and the Feynman rules for finite temperature are applied to give

$$\begin{aligned}
 \Pi_{\mu\nu}^{\text{tad}}(q) &= \text{Diagram} \\
 &= \frac{(\pm)}{L_{\text{loop}}} \frac{1}{\beta} \sum_N \int \frac{d^3\mathbf{p}}{(2\pi)^3} \frac{N(p; \alpha, \beta)}{[p^0{}^2 - E_{\mathbf{p}}^2(m_1)]} V(\mu, \nu; \alpha, \beta) \\
 &\quad \times \beta \delta_{\omega_{n'}, -\omega_n} (2\pi)^3 \delta^{(3)}(\mathbf{q}' - \mathbf{q}).
 \end{aligned} \tag{73}$$

The combination of delta functions

$$\Delta = \beta \delta_{\omega_{n'}, -\omega_n} (2\pi)^3 \delta^{(3)}(\mathbf{q}' - \mathbf{q}) \tag{74}$$

is dimensionless and shows that momentum and temperature are conserved at the vertex. This combination will not be shown explicitly in the expression for the polarisation tensor.

The function summed over is

$$f(p^0) = \frac{X_{\mu\nu}(p)}{[p^0{}^2 - E_{\mathbf{p}}^2(m_1)]}, \tag{75}$$

where

$$X_{\mu\nu}(p) = \frac{(\pm)}{L_{\text{loop}}} \frac{(\pm)}{C_{\text{contour}}} N(p; \alpha, \beta) V(\mu, \nu; \alpha, \beta), \tag{76}$$

and the contour factor and the statistics factor discussed in Section 2.2.3 have been included. The symmetry factor corresponding to the number of permutations of internal lines that can be made for fixed vertices cannot be included until the particle propagating in the loop is specified.

The propagators for the electroweak particles are given in Appendix A.6. When gauge bosons are propagating in the external legs, the symmetries of the electroweak Lagrangian show that only a gauge boson or a Higgs sector boson can

propagate in the loop. The numerator of the propagator for these two cases can be expressed as

$$N(p; \alpha, \beta) = \begin{cases} g_{\alpha\beta} - \frac{p_\alpha p_\beta}{m^2} & \text{one part of gauge boson,} \\ \frac{p_\alpha p_\beta}{m^2} & \text{other part of gauge boson,} \\ -1 & \text{Higgs sector boson,} \end{cases}$$

where the propagator for the gauge boson is split into two parts.

All 4-vertices of the electroweak Lagrangian are independent of momentum. The numerator $N(p; \alpha, \beta)$ for the particle propagating in the loop and the 4-vertex are combined and the α and β indices are contracted to give $X_{\mu\nu}(p)$. As $N(p; \alpha, \beta)$ is in the form shown above, $X_{\mu\nu}(p)$ can be expressed as a combination of $g_{\mu\nu}$ and $p_\mu p_\nu$.

In the right half-plane, the only pole of $f(p^0)$ occurs at $p^0 = E_{\mathbf{p}}(m_1)$ or alternatively, at $p^2 = m_1^2$. Hence, the residue of $f(p^0)$ is

$${}^{p^0=E_{\mathbf{p}}(m_1)}\text{Res} \left[\frac{X_{\mu\nu}(p)}{[p^2 - E_{\mathbf{p}}^2(m_1)]} \right] = \frac{X_{\mu\nu}(p^2=m_1^2)}{2E_{\mathbf{p}}(m_1)}. \quad (77)$$

With the integration over \mathbf{p} , there is the symmetry $\mathbf{p} \rightarrow -\mathbf{p}$. Hence $f(p^0) = f(-p^0)$ and equation (32) yields

$$\frac{1}{\beta} \sum_N f(p^0) = X_{\mu\nu}(p^2=m_1^2) \frac{F(E_{\mathbf{p}}(m_1), \mu_1)}{2E_{\mathbf{p}}(m_1)}, \quad (78)$$

where F is the general distribution function defined in equation (38). The result for the Matsubara sum means that the expression for the polarisation tensor has the form

$$\Pi_{\mu\nu}^{\text{tad}}(q) = \int \frac{d^3\mathbf{p}}{(2\pi)^3} X_{\mu\nu}(p^2=m_1^2) \frac{F(E_{\mathbf{p}}(m_1), \mu_1)}{2E_{\mathbf{p}}(m_1)}. \quad (79)$$

As shown above, $X_{\mu\nu}(p^2=m_1^2)$ can be expressed as

$$X_{\mu\nu}(p^2=m_1^2) = \mathcal{K}_0 g_{\mu\nu} + \mathcal{M}_0 p_\mu p_\nu, \quad (80)$$

where the general constants \mathcal{K}_0 and \mathcal{M}_0 are obtained from the calculation of $X_{\mu\nu}(p)$ for each diagram. These constants are independent of the integration variable \mathbf{p} and may depend on m_1 .

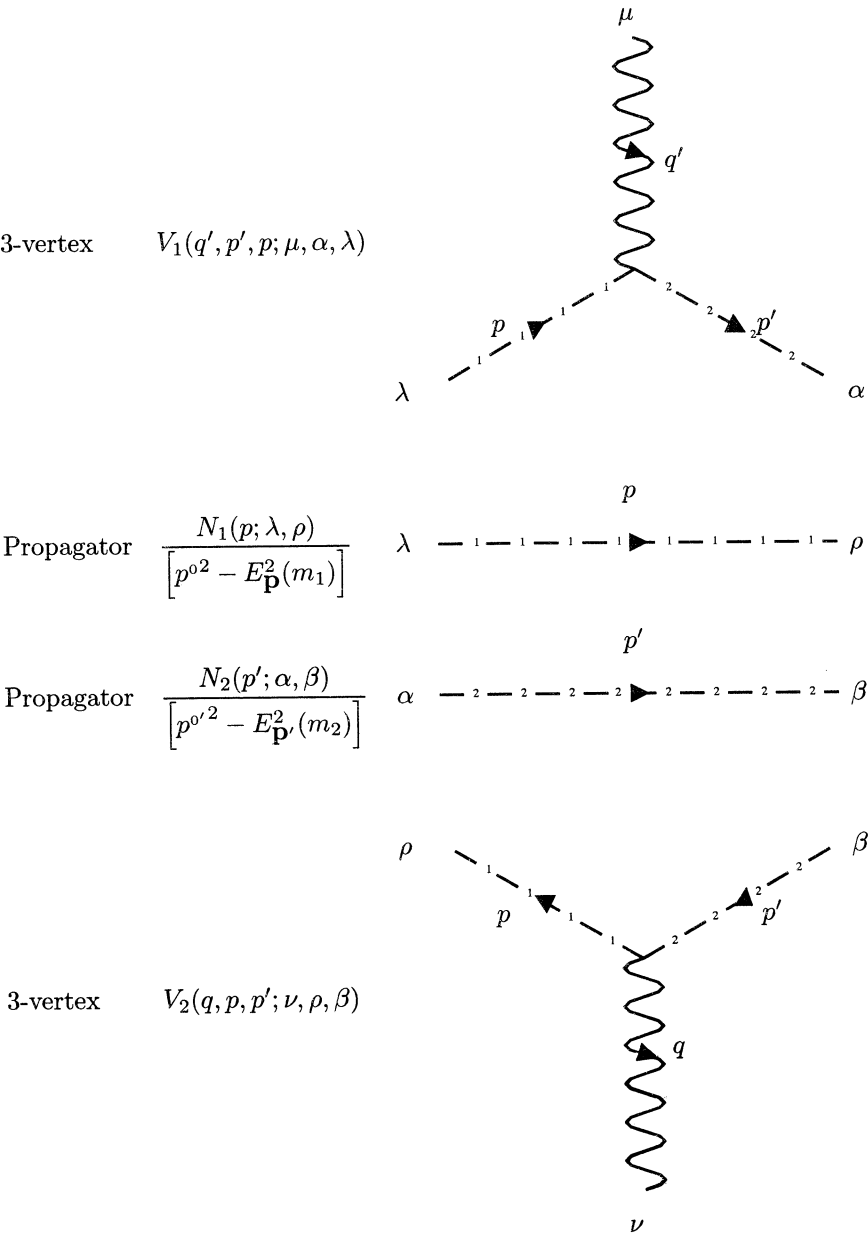
Using this, the generic form for the polarisation tensor for a tadpole diagram is

$$\Pi_{\mu\nu}^{\text{tad}}(q) = \int \frac{d^3\mathbf{p}}{(2\pi)^3} \frac{F(E_{\mathbf{p}}(m_1), \mu_1)}{2E_{\mathbf{p}}(m_1)} (\mathcal{K}_0 g_{\mu\nu} + \mathcal{M}_0 p_\mu p_\nu). \quad (81)$$

This shows that $\Pi_{\mu\nu}^{\text{tad}}(q)$ will be independent of q . In Paper II, the general \mathcal{K}_0 and \mathcal{M}_0 constants are calculated and used with this expression to give the generic form for the polarisation tensor for a tadpole diagram expressed in terms of the polarisation response functions.

5.3 Loop

The loop diagram contains two 3-vertices and two propagators



There are two particles propagating around the loop and they are not necessarily the same. The notation used is that particle 1 is labeled with a '1' on the line and propagates with 4-momentum p , mass m_1 and chemical potential μ_1 . Particle 2 is labeled with a '2' on the line and propagates with 4-momentum p' , mass m_2 and chemical potential μ_2 .

The vertices and propagators for the loop diagram are combined and the Feynman rules for finite temperature are applied. This gives

$$\begin{aligned}
 \Pi_{\mu\nu}^{\text{loop}}(q) = & \text{Diagram: A loop diagram with two wavy external lines. The left wavy line is labeled $(i\omega_{n'} + \mu', \mathbf{q}')$ and the right wavy line is labeled $(i\omega_n + \mu, \mathbf{q})$. The loop consists of two dashed lines. The top dashed line is labeled $(i\omega_{N'} + \mu_2, \mathbf{p}'), m_2$ and the bottom dashed line is labeled $(i\omega_N + \mu_1, \mathbf{p}), m_1$. Arrows indicate the direction of propagation: clockwise for particle 2 and counter-clockwise for particle 1.} \\
 = & \frac{(\pm)}{Loop} \frac{1}{\beta} \sum_N \int \frac{d^3\mathbf{p}}{(2\pi)^3} \frac{1}{\beta} \sum_{N'} \int \frac{d^3\mathbf{p}'}{(2\pi)^3} \frac{N_1(p; \lambda, \rho)}{[p^{02} - E_{\mathbf{p}}^2(m_1)]} \\
 & \times V_1(q', p'; p; \mu, \alpha, \lambda) \frac{N_2(p'; \alpha, \beta)}{[p'^{02} - E_{\mathbf{p}'}^2(m_2)]} V_2(q, p, p'; \nu, \rho, \beta) \\
 & \times \beta \delta_{\omega_{n'} + \omega_N - \omega_{N'}} (2\pi)^3 \delta^{(3)}(\mathbf{q}' + \mathbf{p} - \mathbf{p}') \\
 & \times \beta \delta_{\omega_{N'} - \omega_n - \omega_N} (2\pi)^3 \delta^{(3)}(\mathbf{p}' - \mathbf{q} - \mathbf{p}). \tag{82}
 \end{aligned}$$

If the particles propagating in the loop are fermions, a trace over the gamma matrices is performed. The summation over N' and \mathbf{p}' can be done immediately, yielding $\omega_{N'} = \omega_N + \omega_n$, $\mathbf{p}' = \mathbf{p} + \mathbf{q}$ and the same combination of delta functions as shown in equation (74). For the equilibrium situation considered, $\mu + \mu_1 = \mu_2$, and these relationships are combined to give

$$p^{0'} = i\omega_{N'} + \mu_2 = i\omega_N + \mu_1 + i\omega_n + \mu = p^0 + q^0. \tag{83}$$

The function that has to be summed over is

$$f(p^0) = \frac{X_{\mu\nu}(p)}{[p^{02} - E_{\mathbf{p}}^2(m_1)] [(p^0 + q^0)^2 - E_{\mathbf{p}+\mathbf{q}}^2(m_2)]}, \tag{84}$$

Pole	Residue
$E_{\mathbf{p}}(m_1)$	$\frac{1}{2E_{\mathbf{p}}(m_1)} \frac{X_{\mu\nu}(p; p^0 = E_{\mathbf{p}}(m_1))}{(E_{\mathbf{p}}(m_1) + q^0)^2 - E_{\mathbf{p}+\mathbf{q}}^2(m_2)} n(E_{\mathbf{p}}(m_1) - \mu_1)$
$E_{\mathbf{p}+\mathbf{q}}(m_2) - q^0$	$\frac{1}{2E_{\mathbf{p}+\mathbf{q}}(m_2)} \frac{X_{\mu\nu}(p; p^0 = E_{\mathbf{p}+\mathbf{q}}(m_2) - q^0)}{(E_{\mathbf{p}+\mathbf{q}}(m_2) - q^0)^2 - E_{\mathbf{p}}^2(m_1)} n(E_{\mathbf{p}+\mathbf{q}}(m_2) - \mu_2)$

Table 1: Poles of $f(p^0)n(p^0 - \mu)$ and the residue at these poles

Pole	Residue
$E_{\mathbf{p}}(m_1)$	$\frac{1}{2E_{\mathbf{p}}(m_1)} \frac{X_{\mu\nu}(p; p^0 = -E_{\mathbf{p}}(m_1))}{(E_{\mathbf{p}}(m_1) - q^0)^2 - E_{\mathbf{p}+\mathbf{q}}^2(m_1)} n(E_{\mathbf{p}}(m_1) + \mu_1)$
$E_{\mathbf{p}+\mathbf{q}}(m_2) + q^0$	$\frac{1}{2E_{\mathbf{p}+\mathbf{q}}(m_2)} \frac{X_{\mu\nu}(p; p^0 = -E_{\mathbf{p}+\mathbf{q}}(m_2) - q^0)}{(E_{\mathbf{p}+\mathbf{q}}(m_2) + q^0)^2 - E_{\mathbf{p}}^2(m_1)} n(E_{\mathbf{p}+\mathbf{q}}(m_2) + \mu_2)$

Table 2: Poles of $f(-p^0)n(p^0 + \mu)$ and the residue at these poles

where

$$\begin{aligned}
X_{\mu\nu}(p) = & \left(\begin{smallmatrix} \pm \\ \text{Loop} \end{smallmatrix} \right) \left(\begin{smallmatrix} \pm \\ \text{Contour} \end{smallmatrix} \right) N_1(p; \lambda, \rho) V_1(q, p + q, p; \mu, \alpha, \lambda) \\
& \times N_2(p + q; \alpha, \beta) V_2(q, p, p + q; \nu, \rho, \beta), \tag{85}
\end{aligned}$$

and the loop and statistical factors have already been included.

Now, the Matsubara summation detailed in Section 2.2.3 must be performed. Following equation (37), residues must be evaluated. In the right half-plane the poles of $f(p^0)$ occur at $p^0 = E_{\mathbf{p}}(m_1)$ and $p^0 = E_{\mathbf{p}+\mathbf{q}}(m_2) - q^0$. Evaluating the residues of $n(p^0 - \mu)f(p^0)$ gives the results shown in Table 1. The poles of $f(-p^0)$ occur at $p^0 = E_{\mathbf{p}}(m_1)$ and $p^0 = E_{\mathbf{p}+\mathbf{q}}(m_2) + q^0$. Evaluating the residues of $n(p^0 + \mu)f(-p^0)$ gives the results shown in Table 2.

Now we take the same diagram but with each particle in the loop changed to its own anti-particle. The vertex factors used in the diagram are unchanged. The propagators of the gauge bosons, Higgs sector bosons and ghost particles do not change. The fermion propagator, which depends on \not{p} , does change but as there is a trace over the gamma matrices this change does not affect the form of $X_{\mu\nu}(p)$. Hence the change to the residues is that $\mu_1 \rightarrow -\mu_1, \mu_2 \rightarrow -\mu_2$ and so the residues

for both diagrams taken together have the same form as that shown in Tables 1 and 2, with $n(E_{\mathbf{p}}(m) \pm \mu) \rightarrow F(E_{\mathbf{p}}(m), \mu)$ and with a factor of $\frac{1}{2}$ in front of the combination to avoid double-counting.

The integration variable is \mathbf{p} and so we make the following transformations on each of the 4 residues listed above in the sequence shown below

No change

$$\begin{aligned} \mathbf{p} + \mathbf{q} &\rightarrow \mathbf{p}, & p^0 + q^0 &\rightarrow p^0 & \Rightarrow p &\rightarrow p - q, \\ \mathbf{p} &\rightarrow -\mathbf{p}, & p^0 &\rightarrow -p^0 & \Rightarrow p &\rightarrow -p, \\ \mathbf{p} + \mathbf{q} &\rightarrow -\mathbf{p}, & p^0 + q^0 &\rightarrow -p^0 & \Rightarrow p &\rightarrow -p - q, \end{aligned}$$

Then we have

$$\begin{aligned} \Pi_{\mu\nu}^{\text{loop}}(q) &= \frac{1}{2} \int \frac{d^3p}{(2\pi)^3} \frac{F(E_{\mathbf{p}}(m_1), \mu_1)}{2E_{\mathbf{p}}(m_1)} \left\{ \frac{X_{\mu\nu}(p)}{[(E_{\mathbf{p}}(m_1) + q^0)^2 - E_{\mathbf{p}+\mathbf{q}}^2(m_2)]} \right. \\ &\quad \left. + \frac{X_{\mu\nu}(-p)}{[(E_{\mathbf{p}}(m_1) - q^0)^2 - E_{\mathbf{p}-\mathbf{q}}^2(m_2)]} \right\} \\ &+ \frac{1}{2} \int \frac{d^3p}{(2\pi)^3} \frac{F(E_{\mathbf{p}}(m_2), \mu_2)}{2E_{\mathbf{p}}(m_2)} \left\{ \frac{X_{\mu\nu}(-p - q)}{[(E_{\mathbf{p}}(m_2) + q^0)^2 - E_{\mathbf{p}+\mathbf{q}}^2(m_1)]} \right. \\ &\quad \left. + \frac{X_{\mu\nu}(p - q)}{[(E_{\mathbf{p}}(m_2) - q^0)^2 - E_{\mathbf{p}-\mathbf{q}}^2(m_1)]} \right\}. \end{aligned} \quad (86)$$

The first term in this expression, which depends on $X_{\mu\nu}(p)$ and $X_{\mu\nu}(-p)$ implicitly, has $p^0 = E_{\mathbf{p}}(m_1)$ while the second term, which depends on $X_{\mu\nu}(-p - q)$ and $X_{\mu\nu}(p - q)$ implicitly, has $p^0 = E_{\mathbf{p}}(m_2)$. This expression exhibits the various symmetries expected. If the particles are the same, $m_1 = m_2, \mu_1 = \mu_2$ then $X_{\mu\nu}(p) = X_{\mu\nu}(-p - q)$. The two parts of the expression would then be identical and the $\frac{1}{2}$ removes the double counting.

Under $p^0 = E_{\mathbf{p}}(m_1)$ we have

$$(E_{\mathbf{p}}(m_1) \pm q^0)^2 - E_{\mathbf{p} \pm \mathbf{q}}^2(m_2) = \pm 2(p \cdot q) + (q^2 + m_1^2 - m_2^2), \quad (87)$$

with a similar expression for $p^0 = E_{\mathbf{p}}(m_2)$. Using these expressions the denominators are combined to give

$$\begin{aligned}
\Pi_{\mu\nu}^{\text{loop}}(q) &= \frac{1}{2} \int \frac{d^3p}{(2\pi)^3} \frac{F(E_{\mathbf{p}}(m_1), \mu_1)}{2E_{\mathbf{p}}(m_1)} \left\{ \frac{f_{\mu\nu}(p)}{4(p \cdot q)^2 - (q^2 + m_1^2 - m_2^2)^2} \right\} \\
&+ \frac{1}{2} \int \frac{d^3p}{(2\pi)^3} \frac{F(E_{\mathbf{p}}(m_2), \mu_2)}{2E_{\mathbf{p}}(m_2)} \left\{ \frac{h_{\mu\nu}(p)}{4(p \cdot q)^2 - (q^2 + m_2^2 - m_1^2)^2} \right\},
\end{aligned} \tag{88}$$

where

$$\begin{aligned}
f_{\mu\nu}(p) &= -2(q^2 + m_1^2 - m_2^2) \frac{1}{2} [X_{\mu\nu}(p) + X_{\mu\nu}(-p)] \\
&+ 4p \cdot q \frac{1}{2} [X_{\mu\nu}(p) - X_{\mu\nu}(-p)],
\end{aligned} \tag{89}$$

$$\begin{aligned}
h_{\mu\nu}(p) &= -2(q^2 + m_2^2 - m_1^2) \frac{1}{2} [X_{\mu\nu}(-p - q) + X_{\mu\nu}(p - q)] \\
&+ 4p \cdot q \frac{1}{2} [X_{\mu\nu}(-p - q) - X_{\mu\nu}(p - q)].
\end{aligned} \tag{90}$$

For the case where the particles propagating in the loop are of the same type (e.g. both Higgs sector bosons), $h_{\mu\nu}(p)$ could be obtained from $f_{\mu\nu}(p)$ under $m_1 \leftrightarrow m_2$. The function $X_{\mu\nu}(p)$ is composed of 2 vertex and 2 propagator factors, each of which is dependent on a linear combination of p and q . Due to the contraction on the indices, $X_{\mu\nu}(p)$ can only depend on p^2 , $p \cdot q$, q^2 and pairwise combinations of these. Hence, only the odd part of $X_{\mu\nu}(p)$ will involve $p \cdot q$ or $p_\mu q_\nu + q_\mu p_\nu$ and $f_{\mu\nu}(p)$ and $h_{\mu\nu}(p)$ are expressed in the form

$$\begin{aligned}
f_{\mu\nu}(p) &= [\mathcal{K}_1 + \mathcal{K}_2(p \cdot q)^2] g_{\mu\nu} + [\mathcal{K}_3 + \mathcal{K}_4(p \cdot q)^2] p_\mu p_\nu \\
&+ [\mathcal{K}_5 + \mathcal{K}_6(p \cdot q)^2] q_\mu q_\nu + \mathcal{K}_7 p \cdot q [p_\mu q_\nu + q_\mu p_\nu],
\end{aligned} \tag{91}$$

$$\begin{aligned}
h_{\mu\nu}(p) &= [\mathcal{M}_1 + \mathcal{M}_2(p \cdot q)^2] g_{\mu\nu} + [\mathcal{M}_3 + \mathcal{M}_4(p \cdot q)^2] p_\mu p_\nu \\
&+ [\mathcal{M}_5 + \mathcal{M}_6(p \cdot q)^2] q_\mu q_\nu + \mathcal{M}_7 p \cdot q [p_\mu q_\nu + q_\mu p_\nu].
\end{aligned} \tag{92}$$

The general constants \mathcal{K}_i and \mathcal{M}_i are obtained from the calculation of $f_{\mu\nu}(p)$ and $h_{\mu\nu}(p)$ for each diagram. These constants are independent of the integration variable \mathbf{p} and may depend on m_1 , m_2 and q^2 . The relationship $p^2 = m^2$ under $p^0 = E_{\mathbf{p}}(m)$ has been used.

Where two fermions are propagating in the loop, there is a trace over the gamma matrices. The general form of the vertex involving a gauge boson and two fermions depends on \mathbf{I} and γ_5 hence when the trace is performed, a term $\varepsilon^{\mu\nu\alpha\beta} p_\alpha q_\beta$ arises. This term can be dropped as the final results for the diagram must be symmetric in the μ and ν indices.

The contribution to the polarisation tensor can be simplified using

$$\frac{(p \cdot q)^2}{4(p \cdot q)^2 - (q^2 + m_1^2 - m_2^2)^2} = \frac{1}{4} + \frac{1}{4} \frac{(q^2 + m_1^2 - m_2^2)^2}{4(p \cdot q)^2 - (q^2 + m_1^2 - m_2^2)^2}. \quad (93)$$

Hence, the generic form for the polarisation tensor for a loop diagram is

$$\begin{aligned} \Pi_{\mu\nu}^{\text{loop}}(q) &= \frac{1}{2} \int \frac{d^3\mathbf{p}}{(2\pi)^3} \frac{F(E_{\mathbf{p}}(m_1), \mu_1)}{2E_{\mathbf{p}}(m_1)} \left\{ \frac{1}{4} \mathcal{K}_2 g_{\mu\nu} + \frac{1}{4} \mathcal{K}_4 p_\mu p_\nu + \frac{1}{4} \mathcal{K}_6 q_\mu q_\nu \right\} \\ &+ \frac{1}{2} \int \frac{d^3\mathbf{p}}{(2\pi)^3} \frac{F(E_{\mathbf{p}}(m_1), \mu_1)}{2E_{\mathbf{p}}(m_1)} [4(p \cdot q)^2 - (q^2 + m_1^2 - m_2^2)^2]^{-1} \\ &\quad \times \left\{ [\mathcal{K}_1 + \frac{1}{4} \mathcal{K}_2 (q^2 + m_1^2 - m_2^2)^2] g_{\mu\nu} \right. \\ &\quad + [\mathcal{K}_3 + \frac{1}{4} \mathcal{K}_4 (q^2 + m_1^2 - m_2^2)^2] p_\mu p_\nu \\ &\quad + [\mathcal{K}_5 + \frac{1}{4} \mathcal{K}_6 (q^2 + m_1^2 - m_2^2)^2] q_\mu q_\nu \\ &\quad \left. + \mathcal{K}_7 p \cdot q [p_\mu q_\nu + q_\mu p_\nu] \right\} \\ &+ \frac{1}{2} \int \frac{d^3\mathbf{p}}{(2\pi)^3} \frac{F(E_{\mathbf{p}}(m_2), \mu_2)}{2E_{\mathbf{p}}(m_2)} \left\{ \frac{1}{4} \mathcal{M}_2 g_{\mu\nu} + \frac{1}{4} \mathcal{M}_4 p_\mu p_\nu + \frac{1}{4} \mathcal{M}_6 q_\mu q_\nu \right\} \\ &+ \frac{1}{2} \int \frac{d^3\mathbf{p}}{(2\pi)^3} \frac{F(E_{\mathbf{p}}(m_2), \mu_2)}{2E_{\mathbf{p}}(m_2)} [4(p \cdot q)^2 - (q^2 + m_2^2 - m_1^2)^2]^{-1} \\ &\quad \times \left\{ [\mathcal{M}_1 + \frac{1}{4} \mathcal{M}_2 (q^2 + m_2^2 - m_1^2)^2] g_{\mu\nu} \right. \\ &\quad + [\mathcal{M}_3 + \frac{1}{4} \mathcal{M}_4 (q^2 + m_2^2 - m_1^2)^2] p_\mu p_\nu \\ &\quad + [\mathcal{M}_5 + \frac{1}{4} \mathcal{M}_6 (q^2 + m_2^2 - m_1^2)^2] q_\mu q_\nu \\ &\quad \left. + \mathcal{M}_7 p \cdot q [p_\mu q_\nu + q_\mu p_\nu] \right\}. \quad (94) \end{aligned}$$

In Paper II, the general $\mathcal{K}_{1...7}$ and $\mathcal{M}_{0...7}$ constants are calculated and used with this expression to give the generic form for the polarisation tensor for a loop diagram expressed in terms of the polarisation response functions.

At this point it is worth while pausing to examine the overall features of equation (94). The general constants \mathcal{K}_i and \mathcal{M}_i are obtained from $f_{\mu\nu}(p)$ and $h_{\mu\nu}(p)$, as given in equations (91) and (92). These functions are defined in equations (89) and (90) from $X_{\mu\nu}(p)$, a function given by the contraction of the vertices and the numerators of the propagators of the particles involved as specified by equation (76). This process can be represented as

$$\begin{array}{c} \text{Vertices} \\ \text{Propagators} \end{array} \rightarrow X_{\mu\nu}(p) \rightarrow \frac{f_{\mu\nu}(p)}{h_{\mu\nu}(p)} \rightarrow \frac{\mathcal{K}_i}{\mathcal{M}_i} \rightarrow \Pi_{\mu\nu}^{\text{loop}}(q).$$

As an example, consider the case where a photon is propagating in the external legs and two G^+ bosons are propagating in the loop. Then

$$\begin{aligned} N_1(p; \lambda, \rho) &= -1, \\ V_1(q', p'; p; \mu, \alpha, \lambda) &= -e(p + p')_\mu, \\ N_2(p'; \alpha, \beta) &= -1, \\ V_2(q, p, p'; \nu, \rho, \beta) &= -e(p' + p)_\nu. \end{aligned}$$

The statistical factor is -1 for a boson contour, the loop factor is $+1$ for a boson loop and the symmetry factor is $+1$ as the particles in the loop, although identical, are charged. [Note that G^- is implicitly included in the polarisation tensor.] The numerators and vertices are combined to give

$$X_{\mu\nu}(p) = -e^2 [4p_\mu p_\nu + 2(p_\mu q_\nu + q_\mu p_\nu) + q_\mu q_\nu].$$

Using this expression for $X_{\mu\nu}(p)$ gives

$$\begin{aligned} f_{\mu\nu}(p) &= 2e^2 [4(q^2 + m_1^2 - m_2^2)p_\mu p_\nu - 4p \cdot q (p_\mu q_\nu + q_\mu p_\nu) + (q^2 + m_1^2 - m_2^2)q_\mu q_\nu], \\ h_{\mu\nu}(p) &= f_{\mu\nu}(p) \text{ under } m_1 \leftrightarrow m_2. \end{aligned}$$

This gives for the constants

$$\begin{aligned} \mathcal{K}_3 &= 8e^2(q^2 + m_1^2 - m_2^2), & \mathcal{M}_3 &= 8e^2(q^2 + m_2^2 - m_1^2), \\ \mathcal{K}_5 &= 2e^2(q^2 + m_1^2 - m_2^2), & \mathcal{M}_5 &= 2e^2(q^2 + m_2^2 - m_1^2), \\ \mathcal{K}_7 &= -8e^2, & \mathcal{M}_7 &= -8e^2, \end{aligned}$$

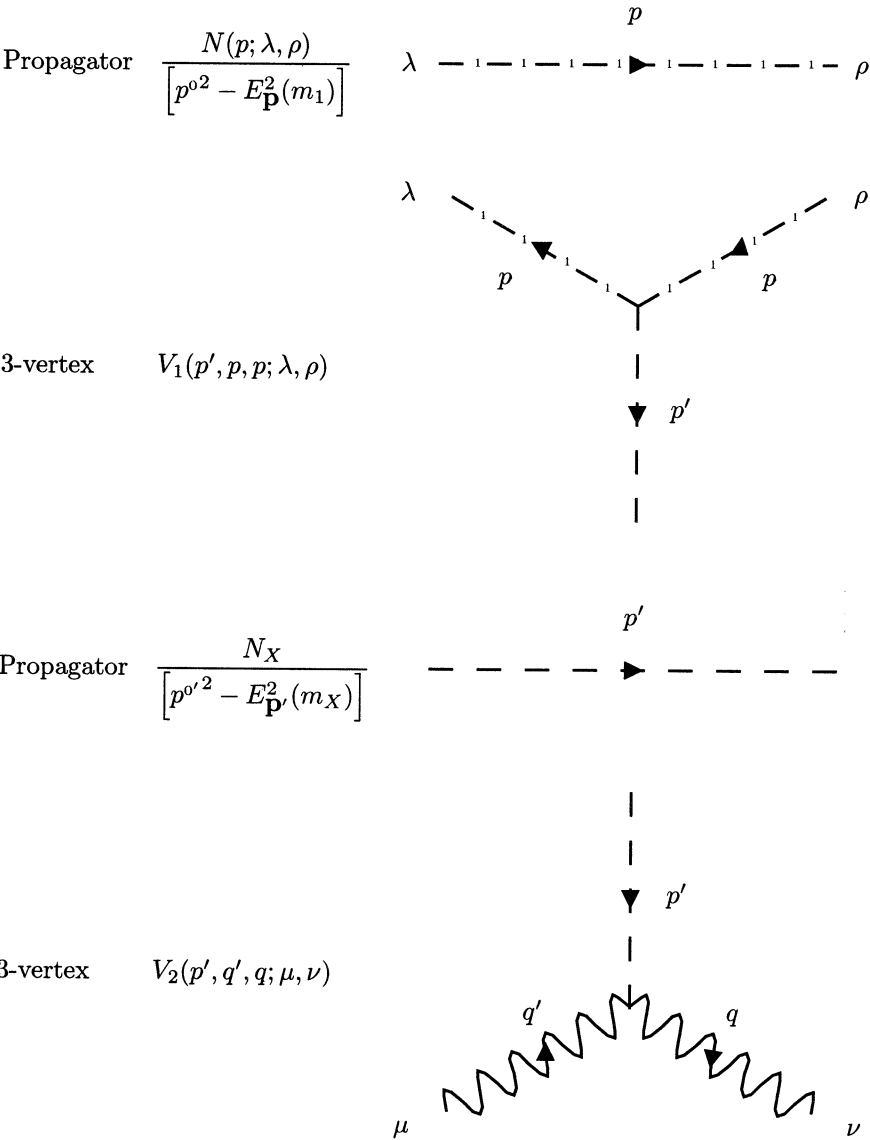
where the \mathcal{K}_i and \mathcal{M}_i constants not explicitly shown are zero. These constants are inserted into the expression given in equation (94) to obtain the polarisation tensor.

This calculation has all been performed with the photon- G^+-G^+ vertex. The usefulness of this arrangement is that the vertex factor for a gauge boson and two Higgs sector bosons has the same general form as the photon- G^+-G^+ vertex, so for the case where a gauge boson and two Higgs sector bosons form the vertex, $-e$ could be replaced by a general factor, say, \mathcal{A}_4 . Hence the polarisation tensor obtained from the calculations given above could be used for the general case with $-e$ replaced by \mathcal{A}_4 . Furthermore, the same process can be followed for a more complicated situation using the general vertex factors given in Section A.7. This method exploits the symmetries of the Lagrangian, reduces the number of calculations required and is applicable to calculations where the vertex factors are

complicated, in particular where two gauge bosons are propagating in the loop. The procedure given above has been used with the computer application Mathematica of Wolfram (1991) and the Mathematica package HIP of Hsieh and Yehudai (1992) to obtain the \mathcal{K}_i and \mathcal{M}_i constants for the most general types of Feynman diagrams. The polarisation response functions given in Paper II explicitly use the results for these constants.

5.4 Balloon

The balloon diagram contains two 3-vertices and two propagators



The particle propagating in the loop has 4-momentum p , with mass m_1 and chemical potential μ_1 . The particle that is exchanged with 4-momentum p' has mass m_X and chemical potential μ_X .

The vertices and propagators for the balloon diagram are combined and the Feynman rules for finite temperature are applied to give

$$\begin{aligned}
 \Pi_{\mu\nu}^{\text{ball}}(q) &= \text{Diagram} \\
 &= \left(\pm \right)_{\text{Loop}} \frac{1}{\beta} \sum_N \int \frac{d^3\mathbf{p}}{(2\pi)^3} \frac{1}{\beta} \sum_{N'} \int \frac{d^3\mathbf{p}'}{(2\pi)^3} \frac{N(p; \lambda, \rho)}{\left[p^0{}^2 - E_{\mathbf{p}}^2(m_1) \right]} \\
 &\quad \times V_1(p', p, p; \lambda, \rho) \frac{N_X}{\left[p'^0{}^2 - E_{\mathbf{p}'}^2(m_X) \right]} V_2(p', q', q; \mu, \nu) \\
 &\quad \times \beta \delta_{\omega_{n'} + \omega_{N'} - \omega_n} (2\pi)^3 \delta^{(3)}(\mathbf{q}' + \mathbf{p}' - \mathbf{q}) \\
 &\quad \times \beta \delta_{\omega_N - \omega_{N'} - \omega_N} (2\pi)^3 \delta^{(3)}(\mathbf{p} - \mathbf{p}' - \mathbf{p}). \tag{95}
 \end{aligned}$$

The summation over N' and \mathbf{p}' is done immediately, yielding $\omega_{N'} = 0$, $\mathbf{p}' = 0$ and the same combination of delta functions as shown in equation (74). This restriction means that a gauge boson cannot be the particle exchanged, as a zero momentum particle cannot carry a Lorentz index. The only uncharged particle that couples to two gauge bosons is the Higgs boson. For $p' = 0$, the Higgs boson propagator reduces to $1/m_H^2$.

The function summed over is

$$f(p^0) = \frac{X_{\mu\nu}(p)}{\left[p^0{}^2 - E_{\mathbf{p}}^2(m_1) \right]}, \tag{96}$$

where

$$X_{\mu\nu}(p) = \frac{(\pm)}{Loop} \frac{(\pm)}{Contour} \frac{1}{m_H^2} V_1(p' = 0, p, p; \lambda, \rho) N(p; \lambda, \rho) V_2(p' = 0, q, q; \mu, \nu), \quad (97)$$

and the contour ‘statistics’ factor has already been included.

In the right half-plane, the only pole of $f(p^0)$ occurs at $p^0 = E_{\mathbf{P}}(m_1)$. The residue of the denominator is the same as in the tadpole case, hence

$$\Pi_{\mu\nu}^{\text{ball}}(q) = \int \frac{d^3\mathbf{p}}{(2\pi)^3} \frac{1}{2E_{\mathbf{P}}(m_1)} \{X_{\mu\nu}(p)n(E_{\mathbf{P}}(m_1) - \mu_1) + X_{\mu\nu}(-p)n(E_{\mathbf{P}}(m_1) + \mu_1)\}. \quad (98)$$

Now we take the same diagram but the particle in the loop changed to its own anti-particle, propagating in the same direction. The vertex factors used in the diagram are unchanged. The propagators of the particles do not change and for the fermion propagator, which depends on \mathbf{p} , there is a trace over the gamma matrices. Hence the form of $X_{\mu\nu}(p)$ does not change. Hence the change to the residues is that $\mu_1 \rightarrow -\mu_1, \mu_2 \rightarrow -\mu_2$ and so the residues for both diagrams taken together have the same form. The polarisation tensor for both diagrams taken together has the form

$$\Pi_{\mu\nu}^{\text{ball}}(q) = \frac{1}{2} \int \frac{d^3\mathbf{p}}{(2\pi)^3} \frac{F(E_{\mathbf{P}}(m_1), \mu_1)}{2E_{\mathbf{P}}(m_1)} \{X_{\mu\nu}(p) + X_{\mu\nu}(-p)\}, \quad (99)$$

where the factor of $\frac{1}{2}$ in front is placed there so that there is no double-counting.

The function $X_{\mu\nu}(p)$ is composed of 2 vertex factors and 2 propagator factors. As the particle exchanged is a Higgs boson the second vertex must be proportional to $g_{\mu\nu}$. The λ and ρ indices are contracted, hence $X_{\mu\nu}(p)$ can only depend on $g_{\mu\nu}$ multiplied by a linear combination of p^2 and q^2 . The residue is evaluated at $p^0 = E_{\mathbf{P}}(m_1)$ which implies that $p^2 = m_1^2$. Hence $X_{\mu\nu}(p)$ can be represented as

$$X_{\mu\nu}(p) = g_{\mu\nu} \mathcal{K}_8, \quad (100)$$

where \mathcal{K}_8 is a general constant. Therefore, the generic form for the polarisation tensor for a balloon diagram is

$$\Pi_{\mu\nu}^{\text{ball}}(q) = \mathcal{K}_8 \int \frac{d^3\mathbf{p}}{(2\pi)^3} \frac{F(E_{\mathbf{P}}(m_1), \mu_1)}{2E_{\mathbf{P}}(m_1)} g_{\mu\nu}. \quad (101)$$

In Paper II, the general \mathcal{K}_8 constants are calculated and used with this expression to give the generic form for the polarisation tensor for a balloon diagram expressed in terms of the polarisation response functions.

6 Summary and Discussion

For the standard electroweak theory (Glashow 1961, Salam 1968, Weinberg 1967), the finite temperature part of the polarisation tensor for the W^\pm , Z^0 and γ gauge bosons has been calculated in a systematic manner using gauge field theory and the R_ξ gauge. The polarisation tensor gives the shift in the propagator of the gauge bosons due to interactions.

Finite temperature field theory is used in the imaginary-time formalism which means that the perturbation expansion used for the zero temperature theory can be carried over to the finite temperature calculations under the application of the finite temperature Feynman rules. These rules prescribe a Matsubara summation due to the periodic boundary conditions.

The contributions to the polarisation tensor due to the interactions described by the electroweak model are expressed in terms of Feynman diagrams. Each Feynman diagram is one of three distinct types—loop, tadpole or balloon—and for each of these types, an algorithm is developed to calculate the contribution of the general diagram.

The work presented here will be developed further in Paper II of this series where the final form for the polarisation tensor will be presented. There an appropriate set of basis tensors will be given and the polarisation tensor derived in this paper will be described by polarisation response functions calculated using these basis tensors. Real and imaginary parts of the polarisation response functions will then be obtained so enabling a preliminary study of the characteristics of the electroweak plasma to be undertaken.

7 Acknowledgments

One of us (BJKS) would like to acknowledge the support of an Australian Post-Graduate Research Award. This work was completed with the assistance of an Australian Research Council award.

References

- Aoki, K., Hioki, Z., Kawabe, R., Konuma, M., and Muta, T. (1982). *Supp. Prog. Th. Phys.* **73**, 1.
- Bailin, D., and Love, A. (1986). 'Introduction to Gauge Field Theory' (Adam Hilger: Bristol). Bernard, C. W. (1974). *Phys. Rev. D* **9**, 3312.
- Boyd, C. G., Brahm, D. E., and Hsu, S. D. H. (1993). *Phys. Rev. D* **48**, 4952.
- Cheng, T.-P., and Li, L.-F. (1988). 'Gauge Theory of Elementary Particle Physics' (Oxford University Press: New York).
- Cole, J. P. (1985). *Prog. Part. & Nucl. Phys.* **12** (Ed. D. Wilkinson), 241.
- Ferrer, E. J., De La Incera, V., and Shabad, A. E. (1987). *Nuovo Cimento A* **98**, 245.
- Ferrer, E. J., De La Incera, V., and Shabad, A. E. (1988). *Nucl. Phys. B* **309**, 120.
- Ferrer, E. J., De La Incera, V., and Shabad, A. E. (1990a). *Int. J. Mod. Phys. A* **5**, 3417.
- Ferrer, E. J., De La Incera, V., and Shabad, A. E. (1990b). *Ann. Phys.* **201**, 51.
- Fetter, A. L., and Walecka, J. D. (1971). 'Quantum Theory of Many Particle Systems' (McGraw-Hill: New York).
- Glashow, S. L. (1961). *Nucl. Phys.* **22**, 579.
- Hsieh, A., and Yehudai, E. (1992). *Comput. Phys.* **6**, 253.
- Itzykson, C., and Zuber, J. B. (1980). 'Quantum Field Theory' (McGraw-Hill: New York).
- Jackson, J. D. (1975). 'Classical Electrodynamics', 2nd ed. (Wiley: New York).
- Kalashnikov, O. K., Razumov, L. V., and Peres-Rojas, H. (1990). *Phys. Rev. D* **42**, 2363.
- Kapusta, J. I. (1981). *Phys. Rev. D* **24**, 426.
- Kapusta, J. I. (1989). 'Finite Temperature Field Theory' (Cambridge University Press:

New York).

- Kapusta, J. I. (1990). *Phys. Rev. D* **42**, 919.
 Landsman, N. P., and van Weert, C. G. (1987). *Phys. Rep.* **145**, 141.
 Mandl, F., and Shaw, G. (1984). 'Quantum Field Theory' (Wiley: New York).
 Melrose, D. B., and McPhedran, R. C. (1993). 'Electromagnetic Processes in Dispersive Media' (Cambridge University Press: New York).
 Morley, P. D., and Kislinger, M. B. (1979). *Phys. Rep.* **51**, 63.
 Pokorski, S. (1987). 'Gauge Field Theories' (Cambridge University Press: New York).
 Salam, A. (1968). In 'Elementary Particle Physics (Nobel Symp. No. 8)' (Ed. N. Svartholm) (Almqvist and Wilsell).
 Smith, B. J. K., Witte, N. S., and Hines, K. C. (1995). *Aust. J. Phys.* **48**, 775.
 Tsyтович, V. N. (1961). *Sov. Phys. JETP* **13**, 1249.
 Weinberg, S. (1967). *Phys. Rev. Lett.* **19**, 1264.
 Williams, D. R. M., and Melrose, D. B. (1989). *Aust. J. Phys.* **42**, 59.
 Witte, N. S. (1990). *J. Phys. A* **23**, 5257.
 Witte, N. S., Dawe, R. L., and Hines, K. C. (1987). *J. Math. Phys.* **28**, 1864.
 Witte, N. S., Kowalenko, V., and Hines, K. C. (1988). *Phys. Rev. D* **38**, 3667; *Errata* **40**, 1370.
 Wolfram, S. (1991). 'Mathematica—A System for Doing Mathematics by Computer', 2nd ed. (Addison-Wesley: Redwood City, California).

A Notation

The notation used in this work is standard (except for the labelling used for the vertices) and is taken from a number of reference works including Mandl and Shaw (1984), Bailin and Love (1986) and in particular Cheng and Li (1988).

A.1 Units

Natural units are used in this work, where $\hbar = c = k_B = 1$. As an example, this gives the fine structure constant as

$$\alpha = \frac{e^2}{4\pi} = \frac{1}{137},$$

so that electric charge is a dimensionless quantity. The energy-momentum relationship for a relativistic particle is given by

$$E_{\mathbf{p}}^2(m) = \vec{p}^2 + m^2,$$

where both momentum and mass are measured in units of energy. The distribution functions become

$$\left[e^{E/T} \pm 1 \right]^{-1} \quad \begin{array}{l} + \text{ Boson/Ghost,} \\ - \text{ Fermion,} \end{array}$$

where temperature is measured in units of energy.

A.2 Metric

$$g^{\mu\nu} = g_{\mu\nu} = \begin{pmatrix} 1 & 0 & 0 & 0 \\ 0 & -1 & 0 & 0 \\ 0 & 0 & -1 & 0 \\ 0 & 0 & 0 & -1 \end{pmatrix},$$

Scalar Product	$A \cdot B = A^\mu B_\mu = A_\mu g^{\mu\nu} B_\nu = A^0 B_0 - \mathbf{A} \cdot \mathbf{B},$
Contravariant Tensor	$q^\mu = (\omega, \mathbf{q}),$
Covariant Tensor	$q_\mu = (\omega, -\mathbf{q}).$

A.3 Pauli Matrices

$$\begin{aligned}\tau_1 &= \begin{pmatrix} 0 & 1 \\ 1 & 0 \end{pmatrix}, \\ \tau_2 &= \begin{pmatrix} 0 & -i \\ i & 0 \end{pmatrix}, \\ \tau_3 &= \begin{pmatrix} 1 & 0 \\ 0 & -1 \end{pmatrix}.\end{aligned}$$

A.4 Dirac Matrices

$$\begin{aligned}\{\gamma_\mu, \gamma_\nu\} &= 2g_{\mu\nu}, \\ \gamma^5 &= \gamma_5 = i\gamma^0\gamma^1\gamma^2\gamma^3, \\ (\gamma^5)^2 &= \mathbf{I}.\end{aligned}$$

A.5 Trace Algebra

$$\begin{aligned}\text{tr}(1) &= 4, \\ \text{tr}(\gamma^5) &= 0, \\ \text{tr}(\text{odd number of matrices}) &= 0, \\ \text{tr}(\gamma^\mu\gamma^\nu) &= 4g^{\mu\nu}, \\ \text{tr}(\gamma^\mu\gamma^5) &= 0, \\ \text{tr}(\gamma^\mu\gamma^\nu\gamma^5) &= 0, \\ \text{tr}(\gamma^\mu\gamma^\nu\gamma^\rho\gamma^5) &= 0, \\ \text{tr}(\gamma^\mu\gamma^\nu\gamma^\rho\gamma^\sigma) &= 4(g^{\mu\nu}g^{\rho\sigma} - g^{\mu\rho}g^{\nu\sigma} + g^{\mu\sigma}g^{\nu\rho}), \\ \text{tr}(\gamma^\mu\gamma^\nu\gamma^\rho\gamma^\sigma\gamma^5) &= -4i\varepsilon^{\mu\nu\rho\sigma}.\end{aligned}$$

A.6 Propagators

The propagators for finite temperature field theory are shown here. These are obtained by removing a factor of $-i$ from the standard zero temperature propagators in the R_ξ gauge. This prescription is given in Section 2.2.2.

$$\begin{aligned}\text{Gauge:} \quad & \left(g_{\alpha\beta} - \frac{p_\alpha p_\beta}{m^2} \right) \left[p^{02} - E_{\mathbf{p}}^2(m) \right]^{-1} + \frac{p_\alpha p_\beta}{m^2} \left[p^{02} - E_{\mathbf{p}}^2(\xi^{\frac{1}{2}}m) \right]^{-1}, \\ \text{Higgs:} \quad & - \left[p^{02} - E_{\mathbf{p}}^2(m) \right]^{-1},\end{aligned}$$

Ghost:
$$-\left[p^{02}-E_{\mathbf{p}}^2(m)\right]^{-1},$$

Fermion:
$$-(\not{p}+m)\left[p^{02}-E_{\mathbf{p}}^2(m)\right]^{-1}.$$

A.7 Vertices

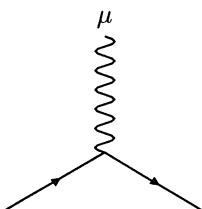
The vertices for the electroweak model are shown here in generic form. Consider the 4-vertex for 2 Higgs sector bosons and 2 gauge bosons. This will always be proportional to $g_{\mu\nu}$. For a specific instance, where 2 G^0 bosons and 2 Z bosons are involved, the constant of proportionality is $i\frac{1}{2}g^2\sec^2\theta_w$. This can be obtained from the electroweak Lagrangian given in Chapter 3 or from most textbooks on gauge field theory, e.g. Bailin and Love (1986), Cheng and Li (1988), Itzykson and Zuber (1980) and Cole (1985) to name a few.

For finite temperature field theory, each vertex loses a factor of i , so for the specific case at finite temperature $C_1 = \frac{1}{2}g^2\sec^2\theta_w$. The generic form is used so that the calculation of the tadpole diagram which depends on the 4-vertex with 2 Higgs sector bosons and 2 gauge bosons, can be performed using the generic factor C_1 and the actual particles involved do not need to be specified. For the particular particles considered above, propagating in the legs of the vertex, $\frac{1}{2}g^2\sec^2\theta_w$ will be inserted in the expression for the diagram in place of C_1 .

A.7.1 3-Vertices

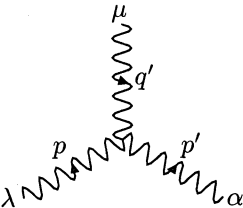
The 3-vertices are arranged to match the labelling used in Section 5.3. The particle labelled with a ‘1’ is on the left-hand side travelling towards the vertex and the particle labelled with a ‘2’ is on the right-hand side travelling towards the vertex.

General form: $\gamma_\mu(\mathcal{A}_0 + \mathcal{A}_1\gamma_5)$



Incoming	1	2	\mathcal{A}_0	\mathcal{A}_1
W^\pm	ν	e^\pm	$-g/(2\sqrt{2})$	$+g/(2\sqrt{2})$
γ	e^\pm	e^\pm	e	0
Z	e^\pm	e^\pm	$g(\frac{1}{4}-\sin^2\theta_w)\sec\theta_w$	$-\frac{1}{4}g\sec\theta_w$
Z	ν	ν	$-\frac{1}{4}g\sec\theta_w$	$+\frac{1}{4}g\sec\theta_w$

Table A1. Gauge-fermion-fermion vertex factors

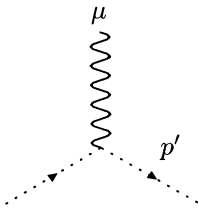


General form: $\mathcal{A}_2 [(-p' - p)_\mu g_{\lambda\alpha} + (p - q')_\alpha g_{\mu\lambda} + (q' + p')_\lambda g_{\alpha\mu}]$

This vertex is symmetric in all particles

Incoming	1	2	\mathcal{A}_2
γ	W^\pm	W^\pm	e
Z	W^\pm	W^\pm	$g \cos \theta_w$

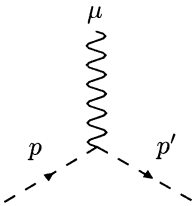
Table A2. Gauge–gauge–gauge vertex factors



General form: $\mathcal{A}_3 p'_\mu$

Incoming	1	2	\mathcal{A}_3
γ	η^+	η^+	$-e$
γ	η^-	η^-	$+e$
Z	η^+	η^+	$-g \cos \theta_w$
Z	η^-	η^-	$+g \cos \theta_w$
W^+	η^-	η^γ	$-e$
W^-	η^+	η^γ	$+e$
W^+	η^-	η^Z	$-g \cos \theta_w$
W^-	η^+	η^Z	$+g \cos \theta_w$
W^+	η^γ	η^+	$-g \sin \theta_w$
W^-	η^γ	η^-	$+g \sin \theta_w$

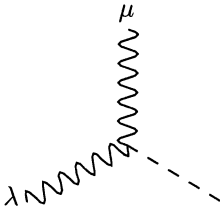
Table A3. Gauge–ghost–ghost vertex factors



General form: $\mathcal{A}_4 (p + p')_\mu$

Incoming	1	2	\mathcal{A}_4
γ	G^+	G^+	$-e$
Z	G^+	G^+	$-g \cos 2\theta_w / (2 \cos \theta_w)$
W^\pm	G^\mp	G^0	$-\frac{1}{2}ig$
W^\pm	G^0	G^\pm	$+\frac{1}{2}ig$
W^\pm	H	G^\pm	$-\frac{1}{2}g$
Z	H	G^0	$-\frac{1}{2}g / \cos \theta_w$

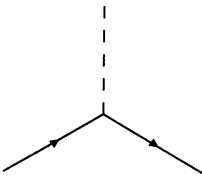
Table A4. Gauge–Higgs–Higgs vertex factors



General form: $\mathcal{A}_5 g_{\mu\lambda}$

Incoming	1	2	\mathcal{A}_5
γ	W^\pm	G^\mp	em_W
Z	W^\pm	G^\mp	$-gm_Z \sin^2 \theta_W$
W^\pm	W^\pm	H	gm_W
Z	Z	H	gm_Z^2/m_W

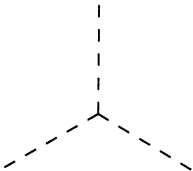
Table A5. Gauge–gauge–Higgs vertex factors



General form: $\mathcal{B}_0 + \mathcal{B}_1 \gamma_5$

Incoming	1	2	\mathcal{B}_0	\mathcal{B}_1
H	e	e	$-\frac{1}{2}gm_e/m_W$	0

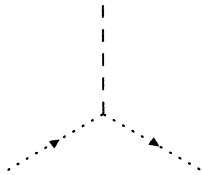
Table B1. Higgs–fermion–fermion vertex factors



General form: \mathcal{B}_2

Incoming	1	2	\mathcal{B}_2
H	G^\pm	G^\pm	$-\frac{1}{2}gm_H^2/m_W$
H	G^0	G^0	$-\frac{1}{2}gm_H^2/m_W$
H	H	H	$-\frac{1}{2}gm_H^2/m_W$

Table B2. Higgs–Higgs–Higgs vertex factors



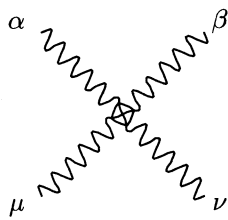
General form: $\mathcal{B}_3\xi$

Incoming	1	2	\mathcal{B}_3
H	η^\pm	$\eta^\pm +$	$-\frac{1}{2}gm_w$
H	η^Z	η^Z	$-\frac{1}{2}m_w \sec^2 \theta_w$

Table B3. Gauge-ghost-ghost vertex factors

A.7.2 4-Vertices

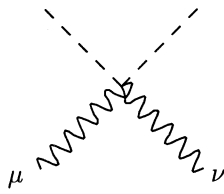
The 4-vertices are



General form: $\mathcal{C}_0 [2g_{\mu\nu}g_{\alpha\beta} - g_{\mu\alpha}g_{\nu\beta} - g_{\mu\beta}g_{\nu\alpha}]$

				\mathcal{C}_0
W^+	W^-	W^+	W^-	g^2
W^+	W^-	γ	γ	$-e^2$
W^+	W^-	Z	Z	$-g^2 \cos^2 \theta_w$

Table C0. Gauge-gauge-gauge-gauge vertex factors



General form: $\mathcal{C}_1 g_{\mu\nu}$

				\mathcal{C}_1
W^+	W^-	G^+	G^-	$\frac{1}{2}g^2$
W^+	W^-	G^0	G^0	$\frac{1}{2}g^2$
W^+	W^-	H	H	$\frac{1}{2}g^2$
Z	Z	G^+	G^-	$\frac{1}{2}g^2 \cos^2 2\theta_w \sec^2 \theta_w$
Z	Z	G^0	G^0	$\frac{1}{2}g^2 \sec^2 \theta_w$
Z	Z	H	H	$\frac{1}{2}g^2 \sec^2 \theta_w$
γ	γ	G^+	G^-	$2e^2$

Table C1. Gauge-gauge-Higgs-Higgs vertex factors